Virology 381 (2008) 89–97

Contents lists available at ScienceDirect

Virology

journal homepage: www.elsevier.com/locate/yviro

Rhesus angiotensin converting enzyme 2 supports entry of severe acute respiratory syndrome coronavirus in Chinese macaques

Yunxin Chen [a,1], Li Liu [b,1], Qiang Wei [a], Hua Zhu [a], Hong Jiang [a], Xinming Tu [a], Chuan Qin [a,*], Zhiwei Chen [b,*]

[a] Institute of Laboratory Animal Science, Chinese Academy of Medical Sciences and Peking Union Medical College, No.5, Panjiayuan, Nanli, Chaoyang District, Beijing, China
[b] AIDS Institute, Li Ka Shing Faculty of Medicine, The University of Hong Kong, 21 Sassoon Road, Pokfulam, Hong Kong, China SAR

ARTICLE INFO

Article history:
Received 4 June 2008
Returned to author for revision 19 July 2008
Accepted 6 August 2008
Available online 17 September 2008

Keywords:
SARS
SARS-CoV
ACE2
Chinese rhesus monkey
Lung pathogenesis

ABSTRACT

Angiotensin converting enzyme 2 (ACE2) is the receptor that severe acute respiratory syndrome coronavirus (SARS-CoV) utilizes for target cell entry and, therefore, plays an important role in SARS pathogenesis. Since Chinese rhesus (rh) macaques do not usually develop SARS after SARS-CoV infection, it has been suggested that rh-ACE2 probably does not support viral entry efficiently. To determine the role of rh-ACE2 in early lung pathogenesis *in vivo*, we studied eleven Chinese rhesus monkeys experimentally infected with a pathogenic SARS-CoV_{PUMC01} strain. Rh-ACE2 genes were amplified from all animals by reverse transcription polymerase chain reaction, and their function was studied *in vitro* using a pseudovirus entry assay. Many natural non-synonymous (NS) changes were found in rh-ACE2 genes. Compared to human (hu) ACE2, thirty-eight consensus NS changes were found in rh-ACE2. Since these changes do not interact with the receptor binding domain of SARS-CoV, rh-ACE2 in general is as effective as human homolog in supporting viral entry. Rh-ACE2, however, is more polymorphic than hu-ACE2. Additional sporadic NS substitutions in clone Rh11-7 reduced the level of rh-ACE2 protein expression and did not support viral entry effectively. Further mutagenesis analysis showed that a natural mutation Y217N dramatically alters ACE2 expression and entry efficiency. Moreover, introduction of the Y217N mutation into hu-ACE2 caused the down-regulation of expression and reduced viral entry efficiency. These results indicate that the Y217N mutation plays a role in modulating SARS-CoV infection. Our results provide insights for understanding the role of rh-ACE2 in SARS lung pathogenesis in a non-human primate model.

Introduction

Severe acute respiratory syndrome (SARS), characterized by pulmonary inflammation and respiratory failure, is an emerging infectious disease caused by a novel coronavirus (CoV) variant, SARS-CoV (Drosten et al., 2003; Kuiken et al., 2003; Peiris et al., 2003a, 2003b). SARS-CoV is highly transmissible in humans with a fatality rate near 10% (Donnelly et al., 2004; Riley et al., 2003). Once infected with SARS-CoV, the typical pathology is severe diffuse alveolar damage (DAD) in patients' lungs, which leads to the failure of lung function (Hamming et al., 2004; Mossel et al., 2005; Nicholls et al., 2003; Tse et al., 2004). Soon after SARS-CoV was isolated, angiotensin-converting enzyme 2 (ACE2) was identified as the primary receptor for SARS-CoV (Li et al., 2003). A recent study of the ACE2 crystal structure revealed that several amino acid residues are very important for binding to the Spike (S) glycoprotein of SARS-CoV (Li et al., 2005b, 2006). Interestingly, individual or an E145/N147/D157 triple mutant in hu-ACE2 had a profound effect on viral entry, which suggested a critical role for ACE2 in SARS-CoV pathogenesis (Han et al., 2006; Hofmann et al., 2006; Li et al., 2005c).

ACE2 was initially identified as an important component of the renin angiotensin system, which controls blood pressure and regulates cardiac function (Crackower et al., 2002). A recent study indicates that ACE2 knockout mice exhibit severe pathology with endotoxin-induced adult respiratory distress syndrome (ARDS) as compared to ACE2 naive mice (Imai et al., 2005). The loss of ACE2 expression in knockout mice results in enhanced vascular permeability, increased lung edema, neutrophil accumulation and weakened lung function. These results indicate that ACE2 plays a protective role in ARDS-related lung damage. Although two studies showed that ACE2 gene polymorphisms do not seem to affect the outcome of SARS in humans (Chiu et al., 2004; Itoyama et al., 2005), a recent small animal study suggests that the down-regulation of ACE2 could contribute to lung damage in a SARS-CoV challenge model (Kuba et al., 2005). Up to now, however, it is still unclear whether a similar mechanism applies to SARS in humans.

Since SARS-CoV cannot be tested in humans, we sought to determine the role of native ACE2 and its variants in lung pathogenesis using

* Corresponding authors. Z. Chen is to be contacted at AIDS Institute, Li Ka Shing Faculty of Medicine, The University of Hong Kong, 21 Sassoon Road, Pokfulam, Hong Kong, China SAR. Fax: +852 2817 7805. C. Qin, Institute of Laboratory Animal Science, Chinese Academy of Medical Sciences and Peking Union Medical College, No.5, Panjiayuan, Nanli, Chaoyang District, Beijing, 100021, P.R. China. Fax: +86 10 67710812.
E-mail addresses: qinchuan@pumc.edu.cn (C. Qin), zchenai@hkucc.hku.hk (Z. Chen).
[1] Contributed equally to this study.

0042-6822/$ – see front matter © 2008 Elsevier Inc. All rights reserved.
doi:10.1016/j.virol.2008.08.016

Table 1
Clinical evaluation of eleven Chinese rhesus monkeys infected with SARS-CoV_{PUMC01} and two uninfected animals

Macaque no.	Gender	Age (years)	Clinical signs	Pathologic examination	IHC[a]	RT-PCR[b]
Rh13	Female	2.5	–	Normal	–	–
Rh14	Male	2.5	–	Normal	–	–
Rh1	Female	2.5	Loss of appetite, Agitated, Aggressive	Mild IP	+	7.1×10^1
Rh6	Male	2.5	Loss of appetite	Mild IP	+	7.1×10^1
Rh7	Female	2.5	Loss of appetite	Mild IP	+	+
Rh9	Female	3.0	Loss of appetite	Mild IP	+	1.6×10^2
Rh10	Male	2.5	Loss of appetite	Mild IP	+	1.5×10^3
Rh12	Male	3.2	–	Mild IP	+	2.7×10^2
Rh2	Male	4.0	Loss of appetite	Severe IP with DAD	+	+
Rh3	Female	3.0	Little movement, Dyspnea	Severe IP with DAD	+	4.0×10^3
Rh4	Male	2.5	Loss of appetite	Severe IP with DAD	+	1.6×10^2
Rh8	Male	3.0	Loss of appetite, Agitated, Aggressive	Severe IP with DAD	+	7.1×10^1
Rh11	Female	2.5	Loss of appetite, Agitated, Aggressive	Severe IP with DAD	+	+

IP represents interstitial pneumonia while DAD is diffuse alveolar damage. The infected monkeys were challenged with 1 ml of 10^5 $TCID_{50}$ of SARS-CoV_{PUMC01} via intranasal route as previously described (Chen et al., 2005).
[a] IHC stands for immunohistochemical staining.
[b] The pharyngeal swap samples were collected at day 5 post infection for the detection of viral RNA by RT-PCR. Rhesus (Rh) monkeys 13 and 14 are uninfected controls.

a SARS-CoV/Chinese monkey model. This model was initially established to investigate the causative agent of SARS and has since played an essential role for testing new strategies for therapies and vaccines against SARS-CoV infection (Chen et al., 2005; Li et al., 2005a; Qin et al., 2005). During these studies, however, we found that Chinese macaques often recover from the viral infection spontaneously and, therefore, never died of SARS. Moreover, the severity of lung damage varies significantly in infected Chinese rhesus monkeys as determined by pathological analysis. Some monkeys developed severe lung damage with DAD while others only had mild interstitial pneumonia. These findings prompted us to examine whether rh-ACE2 could play a role in early lung pathogenesis in these animals.

Results

Lung pathology of Chinese rhesus monkeys infected with the pathogenic SARS-CoV_{PUMC01}

To study the relationship between ACE2 variation and lung damage, we first evaluated the pathologic changes in eleven Chinese rhesus monkeys (Rh1–Rh12) experimentally infected with SARS-CoV_{PUMC01} (Table 1). Two uninfected monkeys (Rh13 and Rh14) were included as controls. Although infected macaques did not have significant clinical signs other than fever and loss of appetite, it was crucial to determine whether they had developed any pathological changes in their respiratory system. For this reason, necropsy specimens collected from the sacrificed macaques were evaluated for pathological abnormalities on day 7 post infection. We chose day 7 for sampling because obvious pathological changes were often found in most infected animals at this time point (Chen et al., 2005; Li et al., 2005a; Qin et al., 2005). In general, the major histopathological changes were primarily found in the lung of infected macaques (Figs. 1B, C, E and F). The infected animals had acute interstitial pneumonia and bronchopneumonia. It was common to see multifocal pulmonary consolidations characterized by broadened alveolar septa, poorly preserved alveolar lining, epithelial hyperplasia, capillary vessel dilation and congestion, and interstitial mononuclear inflammatory cell infiltration. According to the severity of the pathologic changes, six monkeys (Rh1, 6, 7, 9, 10 and 12) were classified in the "mild" group (Figs. 1B and E) with

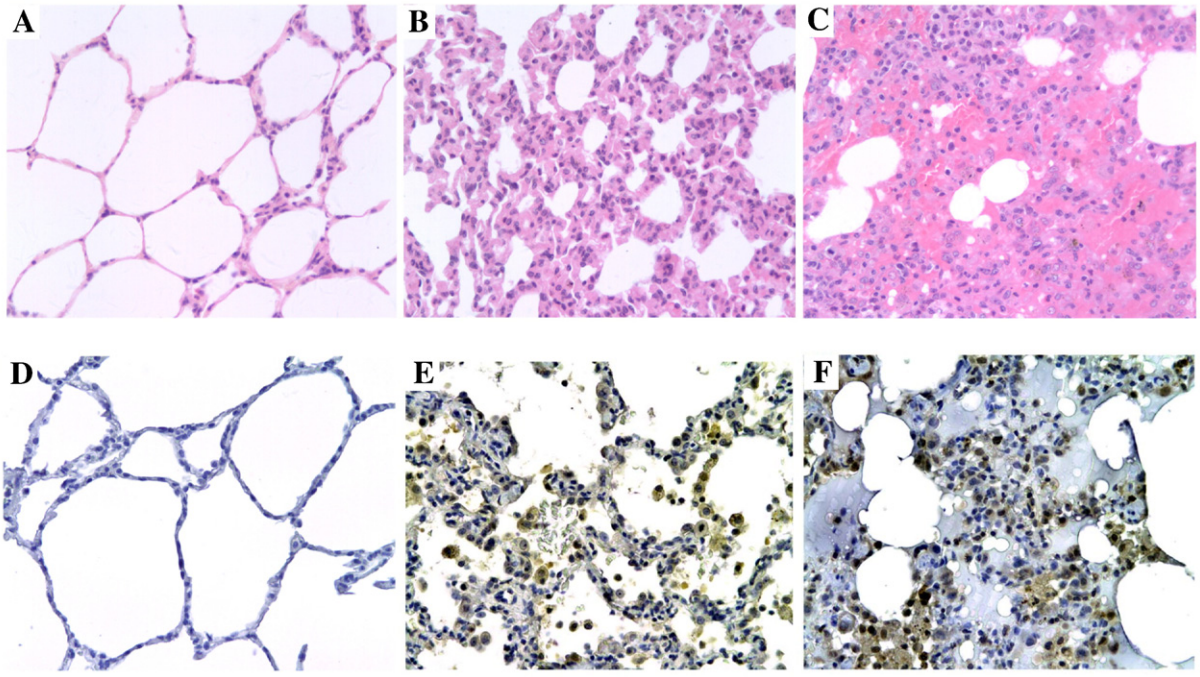

Fig. 1. Pathological evaluation of lung specimens of Chinese rhesus monkeys. Necropsy tissue samples were collected from normal (Rh13, A and D) and SARS-CoV_{PUMC01} infected (Rh1, B and E; Rh11, C and F) animals (Table 1). Data based on H.E. (top panel) and immunohistochemical (bottom panel) staining assays are depicted here with 200x magnification. Macaque Rh1 represents a mild case of infection with thickened alveolar septa and some monocyte infiltration (B and E). Macaque Rh11 represents a severe case of acute DAD with extensively broadened alveolar septa, increased monocyte infiltration, visible exudation of protein-rich edema fluid in alveolar cavities, ruptured elastic alveolar fibers, and local fusion of thick septa (C and F). SARS-CoV specific viral antigens were detected in the lung of both mild and severe animals. Neither pathological changes nor viral antigens were detected in the control animals (A and D).

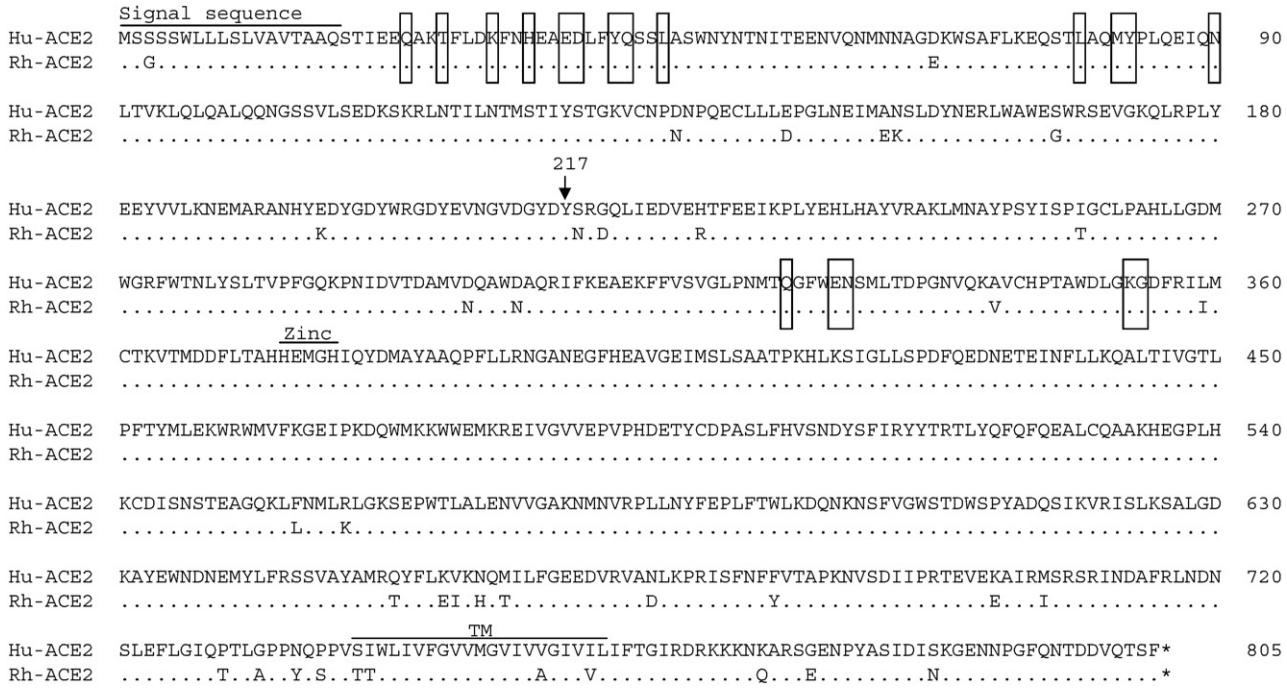

Fig. 2. Consensus sequence alignment of human and Chinese rhesus ACE2. Nucleotide sequences of ACE2 cDNAs were derived from animals Rh1–Rh14 by RT-PCR. Rhesus sequences were compared to seven human homologues in GenBank (accession numbers BC048094, BC039902, AB193260, NM_021804, AB193259, AY358714 and AB046569). Identical amino acids are indicated by dots whereas differences are shown in uppercase. Critical residues, which likely interact with the RBD of SARS-CoV, are indicated by boxes. Signal sequence, zinc domain and transmembrane (TM) region are highlighted with solid lines. The arrow indicates the key residue Y217 which is crucial for ACE2 expression and viral entry.

another five animals (Rh2, 3, 4, 8 and 11) in the "severe" group (Figs. 1C and F). Animals in the latter group developed acute DAD with extensively broadened alveolar septa, increased monocyte infiltration, visible exudation of protein-rich edema fluid in alveolar cavities, ruptured elastic fiber of alveolus, and local fusion of thick septa (Figs. 1C and F). In contrast, uninfected animals did not display signs of lung damage (Figs. 1A and D). SARS-CoV specific antigens were detected in both groups of infected animals (Figs. 1E and F).

Natural variation of rh-ACE2 genes among infected monkeys

To understand the role of rh-ACE2 variation in the observed lung pathology, the genes of rh-ACE2 were amplified from all animals and subsequently sequenced. High fidelity Taq-polymerase was used to minimize the sequence error generated during amplification. Based on the comparison of amino acid sequences, we found that there are 38 differences between the hu- and rh-ACE2, which gave an overall homology of 91% (Fig. 2 and Table 2). These amino acids are probably not making direct contacts with the receptor-binding domain (RBD) of SARS-CoV because they are not the interacting sites previously identified (Fig. 2).

Furthermore, there are also 47 sporadic non-synonymous (NS) variations in rh-ACE2 genes, which are rarely found in hu-ACE2 (Fig. 3). The G466D mutation was found in half of the animals, but did not correlate with the severity of lung damage. Sequence analysis shows that hu-ACE2 genes are less diverse with an average intraspecies genetic homology of 99.9%, which contrasts the 99.1% found in Chinese monkeys (Table 2). Pairwise comparison indicates that the average ds/dn of rh-ACE2 (3.6689) is significantly smaller than that of hu-ACE2 (10.4417) (Table 2). Multiple ACE2 clones from each animal were sequenced with consistent variations obtained. Interestingly, none of these sporadic NS mutations make critical interactions with the RBD (Figs. 2 and 3). Therefore, the deduced RBD binding residues in ACE2 are highly conserved between human and Chinese rhesus homologues (Fig. 2). Moreover, the zinc domain which is crucial for the catalytic activity of ACE2 is also conserved.

Table 2
Sequence homology between human and Chinese rhesus ACE2 (%)

Gene	Hu-ACE2		Rh-ACE2	
	Amino acid	Nucleotide[a]	Amino acid	Nucleotide
Hu-ACE2	99.9	99.9	91.0	96.8
Rh-ACE2	91.0	96.8	99.1	99.7

[a] Based on Kimura's two-parameter formula. Averages of all pairwise comparisons for Rh-ACE2: ds = 0.0061, dn = 0.0023, ds/dn = 3.6689, ps/pn = 3.6553, while for Hu-ACE2: ds = 0.0060, dn = 0.0006, ds/dn = 10.4417, ps/pn = 10.4043.

Expression of rh-ACE2 in human cells

Since sporadic NS mutations were found in the rh-ACE2 gene of each animal, we evaluated the expression of these variants in human cells. After HEK293T cells were transfected with an individual plasmid, the ACE2 expression was determined using both western blot and immunofluorescence staining assays. As shown in Fig. 4A, western blot analysis showed that ACE2 expression of all clones was readily detectable except for clones 11-7 derived from macaque Rh11 (Fig. 4A). Moreover, the immunofluorescence assay confirmed that there were a significantly lower number of ACE2 expressing cells when transfected with clone 11-7, which is consistent with the reduced level of ACE2 expression observed in the Western blot analysis.

Rh-ACE2 supports viral entry

Since there are many NS differences between hu-ACE2 and rh-ACE2 genes, we sought to determine how efficient rh-ACE2 would support viral entry. According to the sequence data, we tested every rh-ACE2 clone that contains unique natural mutations. Five nanograms (based on p24) of pseudovirus was used to infect HEK293T cells transfected with an individual rh-ACE2 expression plasmid. As shown in Fig. 4B, all rh-ACE2 variants support viral entry efficiently except for clone 11-7. Interestingly, the level of ACE2 expression was positively

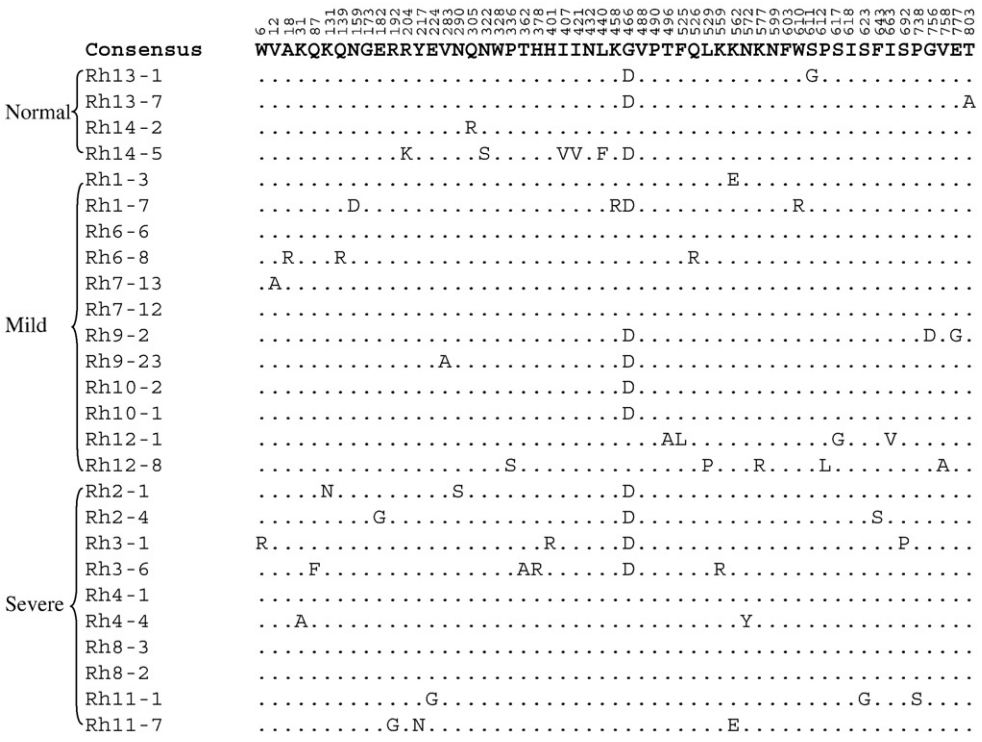

Fig. 3. Sporadic differences between human consensus and individual rhesus ACE2 protein sequence. Identical amino acids are indicated by dots whereas differences are shown in uppercase. The numbers on top of the alignment stand for the positions of each individual variation in ACE2 protein sequence. Animals are divided into three groups as indicated by the severity of lung damage (Fig. 1 and Table 1). These variations were confirmed by sequencing at least three molecular clones from each animal. Two rh-ACE2 clones from each macaque are presented here (e.g. Rh13-1 stands for clone one of rhesus macaque number 13).

correlated with the efficiency of viral infection using the Pearson correlation analysis (r=0.62, p<0.01) (Fig. 4C).

Critically, we further compared the levels of rh-ACE2 expression and viral entry between mild and severe groups of infected animals. As depicted in Fig. 4D, monkeys with mild lung damage had relatively higher levels of rh-ACE2 mRNA expression compared to those in the severe group (t test, p<0.05). Of note, the rh-ACE2 mRNA ratio of Rh11 is 0.05 which is lower than the average value of the severe group (Fig. 4D). Importantly, rh-ACE2 with consensus NS differences supports viral entry as efficiently as hu-ACE2 (Fig. 4E). Therefore, rh-ACE proteins except for Rh11-7 serve as an effective receptor for SARS-CoV entry.

Mutation Y217N reduced the levels of rh-ACE2 expression and viral entry

To identify the key residues which may determine the levels of rh-ACE2 expression and viral entry, we studied the difference between pairs of rh-ACE2 genes in each animal. Since there was over 20-fold difference between clones 11-1 and 11-7 (Fig. 4B), we further conducted mutagenesis on this pair. By analyzing the profiles of all rh-ACE2 clones in mediating viral entry, we found that there were two dominant amino acid differences between clones 11-1 and 11-7, R192G and Y217N (Fig. 5A), which might contribute to the unique phenotype of 11-7. For this reason, individual amino acid substitutions (G192R and N217Y) were introduced into clone 11-7. Interestingly, no significant difference was found in ACE2 expression between 11-7 and 11-7(G192R) using western blot and immunofluorescence assays (Figs. 5B and D). The 11-7(N217Y) mutation, however, was able to restore the expression of 11-7 approaching the level of 11-1 (Fig. 5B). This increase is highly significant (t test, p<0.01). Accordingly, 11-7 (N217Y) also supported viral entry efficiently (Fig. 5C). Therefore, the natural mutation at position 217 likely plays a critical role in controlling the levels of rh-ACE2 expression and viral entry.

Mutation Y217N affects the levels of hu-ACE2 expression and viral entry

To further determine whether the Y217N mutation would play a role in hu-ACE2 expression and viral entry, we generated a hu-ACE2 (Y217N) mutant. Similar to the findings with rh-ACE2 variants, hu-ACE2(Y217N) displayed significantly reduced levels of protein expression and viral entry (Figs. 6A and B; t test, p<0.05). Therefore, although the amino acid Y217 does not make a direct contact with RBD, it is still a critical residue for hu-ACE2 expression and viral entry.

Discussion

In this study, we characterized the function of ACE2 genes derived from eleven Chinese rhesus monkeys experimentally infected with the pathogenic SARS-CoV$_{PUMC01}$ strain. We found that there are 38 (out of 805, 4.7%) consensus non-synonymous substitutions in rh-ACE2 when compared with the consensus human homologue. These substitutions, however, are not involved in viral interaction and, therefore, do not affect the function of rh-ACE2 in mediating SARS-CoV S-glycoprotein dependent viral entry. We, however, show that some sporadic natural non-synonymous mutations are likely critical for rh-ACE2 expression, which, in turn, affects viral infection significantly. In particular, a single amino acid substitution Y217N almost abolishes rh-ACE2 expression and viral entry. This substitution also has a similar effect on the function of hu-ACE2. These results indicate that the natural mutation Y217N in rh-ACE2 probably play a role in modulating the SARS-CoV infection. Our findings, therefore, have implications for understanding the biological function of rh-ACE2, and the role of its natural mutation in SARS-CoV pathogenesis.

Chinese rhesus monkeys display different profiles of lung damage during the acute phase of infection. The predominant pattern of lung injury in most acute human cases that end in fatality includes severe

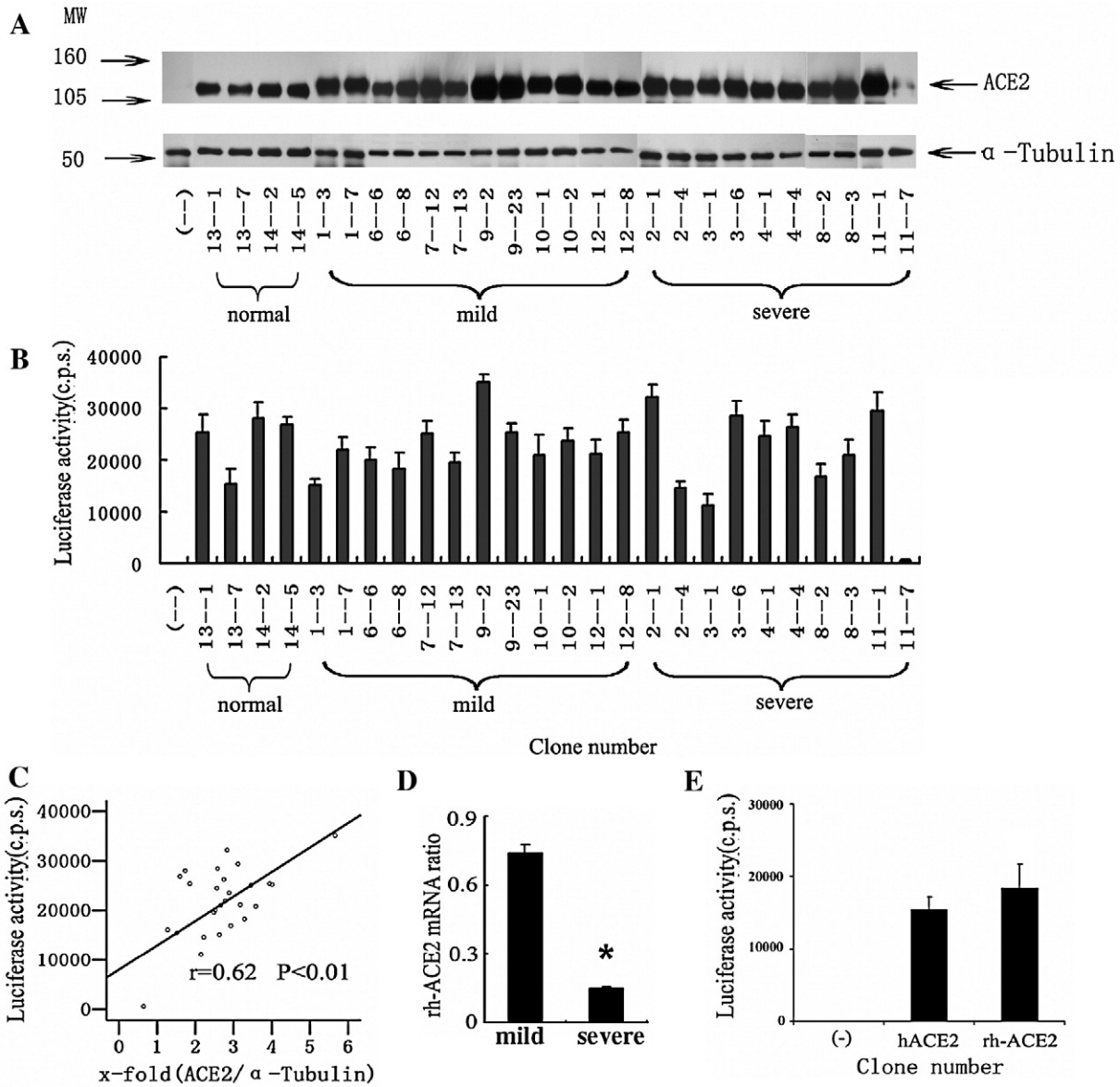

Fig. 4. Natural mutations affect rh-ACE2 expression and viral entry. (A) Rh-ACE2 expression was detected in HEK293T cells transfected with various plasmids by the Western blot analysis. The α-tubulin was used as an internal control. (B) Most rh-ACE2 clones, except for 11-7, supported viral entry into HEK293T cells transfected with corresponding plasmids in a pseudovirus infection assay. The data were confirmed in two experiments and quadruplicates were tested at each time. Error bars indicate standard deviations. (C) The efficiency of viral entry positively correlated with the level of rh-ACE2 expression with an *R* value of 0.624 ($p<0.01$). The level of protein expression was determined by the ratio of OD(ACE2)/OD (α-Tubulin) using Bandscan Software. (D) As indicated by the asterisk, the average level of rh-ACE2 expression in lung specimens was significantly different between the mild and the severe groups (*t* test, $p<0.05$). The ratio is based on calculations using the average level of rh-ACE2 expression of normal macaques as a baseline. (E) The average level of viral entry mediated by consensus rh-ACE2 (clones 8-2 and 8-3 in Fig. 3) is higher than that of hu-ACE2 (*t* test, $p<0.05$).

diffuse alveolar damage (DAD), airspace edema, and bronchiolar fibrin (Franks et al., 2003). Moreover, some cases also exhibit organizing-phase DAD, type II pneumocyte hyperplasia, squamous metaplasia, multinucleated giant cells, and acute bronchopneumonia (Nicholls et al., 2003; Shieh et al., 2005). In previous studies, it has been reported that various species of rhesus macaques can be infected by SARS-CoV (Osterhaus et al., 2004; Qin et al., 2005; Rowe et al., 2004). The infected animals, however, often recovered from viral infection spontaneously and, therefore, never died of SARS. The underlying mechanism which contributes to the disease progression remains unknown in macaques. In this study, we show that eleven macaques were successfully infected with SARS-CoV$_{PUMC01}$, determined mainly by lung pathology, RT-PCR and immunohistochemical staining assays. The challenged macaques were sacrificed on day seven post infection so that the acute lung damages were captured for analysis. Consistent with previous findings in simian models, SARS-CoV infection indeed caused DAD, broadening alveolar septa with increased monocyte infiltration, visible exudation in alveolar cavities, ruptured elastic alveolar fibers, and local fusion of thick septa in Chinese macaques (Figs. 1C and F) (Li et al., 2005a; Qin et al., 2005). However, only a portion of infected animals developed "severe" lung damage with DAD while others only had "mild" interstitial pneumonia based on pathological evaluations (Table 1 and Fig. 1). This finding laid the foundation for further investigation of the function of rh-ACE2 in mediating lung damage.

The viral entry efficiency mediated by rh-ACE2 is unlikely associated with the severity of lung damage in infected Chinese rhesus monkeys. We determine whether the variation of rh-ACE2 plays a role in SARS lung pathogenesis because ACE2 is the primary receptor for SARS-CoV entry into target cells. A recent study indicated that

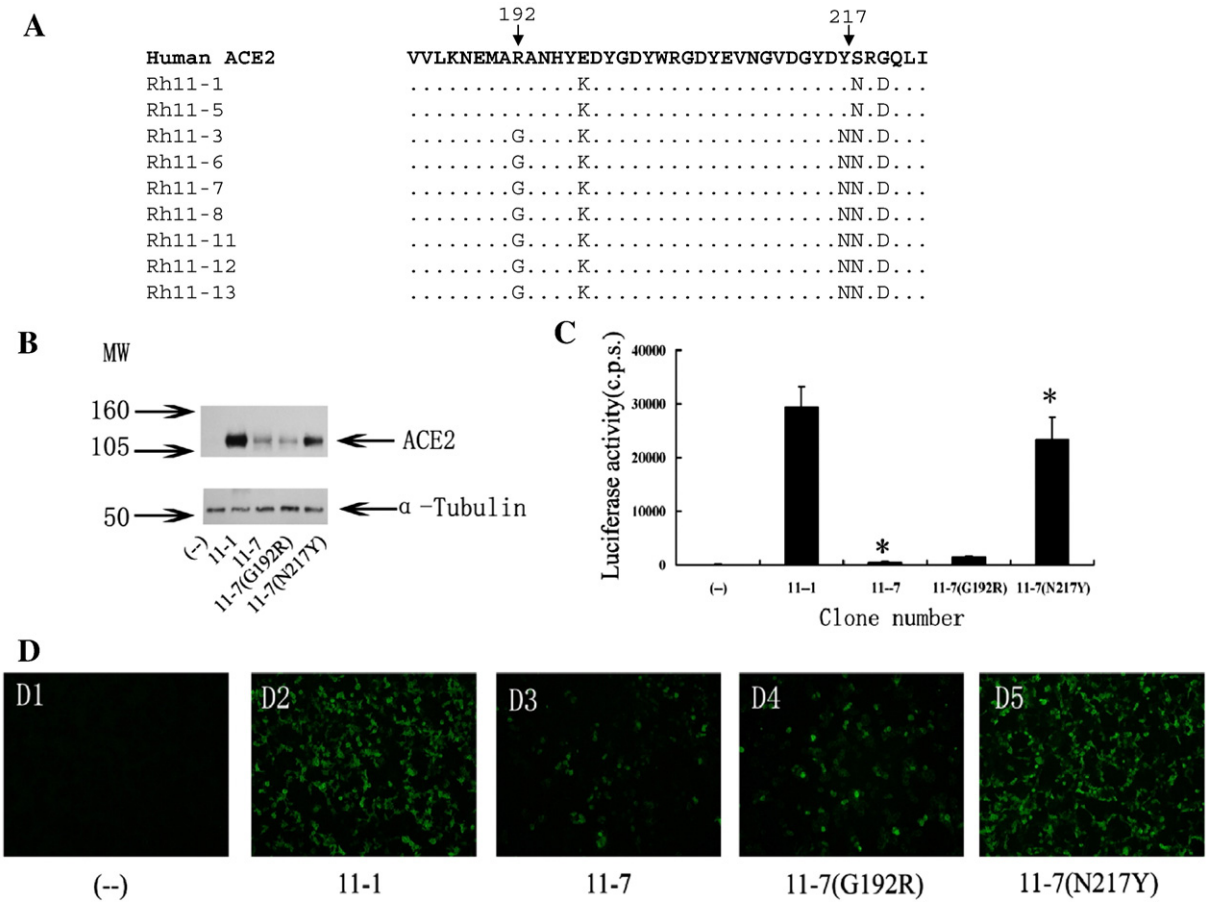

Fig. 5. Influence of a single natural mutation on rh-ACE2 expression and viral entry. (A) The Y217N mutation is found in seven of nine ACE2 clones of monkey Rh11. The arrows indicate the major variations in the selected region of rh-ACE2. (B) Various levels of wild type or mutant rh-ACE2 expression were determined by the Western blot analysis. The positions of rh-ACE2 and α-Tubulin are indicated by arrows. The negative control is HEK293T cells transfected with the pVAX vector alone. Three experiments were conducted with similar results obtained. (C) The levels of viral entry were determined by a pseudotyped infection assay. The left asterisk indicates a significant difference between clones 11-1 and 11-7 on viral entry ($p<0.01$). The right asterisk indicates that the N217Y mutation restores the level of viral entry significantly as compared to clone 11-7 (t test, $p<0.01$). Error bars indicate standard deviations. (D) Various levels of wild type or mutant rh-ACE2 expression were determined by an immunofluorescence staining assay using a goat anti-human-ACE2 polyclonal antibody. Original magnification, ×100.

ACE2 was detected in ciliated epithelial cells of human airway tissues derived from nasal or tracheobronchial regions. It was evident that SARS-CoV may infect the proximal airways and cause highly cytolytic effects because infected ciliated cells were necrotic and shed over time onto the luminal surface of the airway (Sims et al., 2005). Since the ciliated epithelial cells of monkey airway tissues are less susceptible to infection (Sims et al., 2005), it is possible that rh-ACE2 or its variant does not function as an effective receptor for SARS-CoV, which, in turn, leads to a mild disease outcome (Rowe et al., 2004). We, however, found that most rh-ACE2 genes supports viral entry effectively even if they contain 38 or more NS differences when compared with human counterparts (except for clone 11-7) (Figs. 2, 3 and 4B). Based on the sequence of Rh8, which harbors consensus NS differences (Fig. 3), rh-ACE2 supported viral entry with

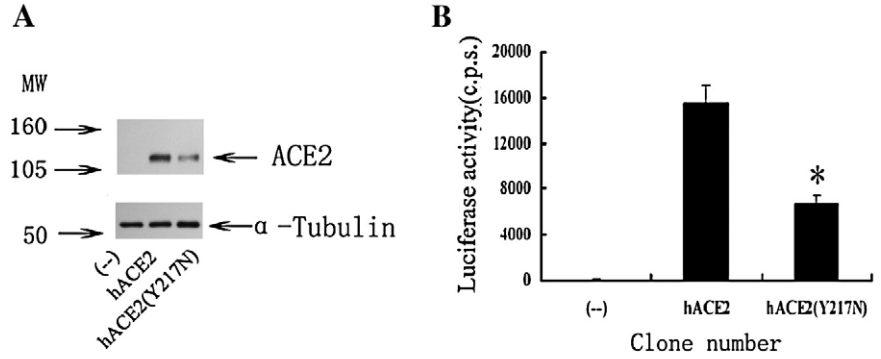

Fig. 6. Y217N mutation reduces the levels of hu-ACE2 expression (A) and viral entry significantly (B). (A) The level of rh-ACE2 expression was determined by the Western blot analysis. The positions of hu-ACE2 and α-Tubulin are indicated by arrows. Three experiments were conducted with similar results. (B) The asterisk indicates a significant difference between hu-ACE2 and hu-ACE2(Y217N) in mediating viral entry. Error bars indicate standard deviations.

slightly better efficiency than the human homologue (Fig. 4E). We therefore believe that, in general, rh-ACE2 itself is not likely acting as a major restriction factor for the self-limiting infection of SARS-CoV in macaques. To this end, other factors involved in lung pathology should be further studied in the model system because previous studies have demonstrated that multiple factors could have contributed to the lung damage of infected SARS patients. These factors include the involvement of other host proteins (e.g. L-SIGN), activation of pro-inflammatory cytokines, improper treatment, and manifestations in multiple organs (Chan et al., 2006; Ding et al., 2004; He et al., 2006; Huang et al., 2006; Law et al., 2005; Peiris et al., 2004; To et al., 2004).

The natural variation of rh-ACE2 genes is relatively diverse among Chinese rhesus monkeys. When compared with seven hu-ACE2 genes deposited in GenBank (Table 2), it is interesting that the sequence homology among rh-ACE2 genes is smaller than that of hu-ACE2. In particular, except for Rh8 and Rh10, most animals harbor heterozygous ACE2 genes with distinct NS substitutions (Table 1; Fig. 3). Moreover, rh-ACE2 has a significantly smaller ds/dn ratio than hu-ACE2 (Table 2). This is unusual compared to monkey chemokine receptor CCR5 and CXCR4, which are often homozygous genes except for the heterozygous variants found in some mangabey species (Chen et al., 1997, 1998a, 1998b). The underlying mechanism driving rh-ACE2 evolution is, therefore, an interesting area for further investigation. We report here a Chinese rhesus monkey that harbors an rh-ACE2 mutant (Rh11-7) which neither expresses well nor supports viral entry efficiently. Since this case was both found among the "severe" groups, it raises one potential hypothesis that this variant might arise due to SARS-CoV infection, and the reduced ACE2 expression, in turn, contributes to severe lung damage (Fig. 4D). Knockdown of ACE2 expression has previously been identified as a causative agent for lung damage in a small animal study, lending further support to this hypothesis (Imai et al., 2005). We found that infected macaques with severe lung damage had significantly lower levels of ACE2 mRNA when compared to the mild group of animals (Fig. 4D). This finding is probably due to the overall damage of lung tissues, which resulted in the significant loss of ACE2 expressing pneumocytes (Figs. 1C and F), rather than to the emergence of Rh11-7 mutant. Detailed studies may require *in vivo* monitoring of rh-ACE2 mRNA levels and protein expression in the lung of infected monkeys over the course of infection, which is technically difficult. Since most NS variations seem to be sporadic (Fig. 3), there is probably not a common mechanism for knock down of rh-ACE2 expression in these animals.

A single, natural mutation in rh-ACE2 gene can determine the entry efficiency of SARS-CoV. A recent structural analysis of hu-ACE2 has identified the key residues that make direct contact with the RBD including Q24, T27, K31, H34, E37, D38, Y41, Q42, L45, L79, M82, Y83, N90, Q325, E329, N330, K353 and G354 (Fig. 2). Interestingly, these sites are located in three discontinuous regions (i) residues K31 and Y41 on α-helix 1; (ii) M82, Y83 and P84 on loop 2; and (iii) K353, D355 and R357 on β-sheet 5 (Li et al., 2005b, 2005c). Mutagenesis studies further indicate that individual substitution of these sites or a triple mutant E145/N147/D157A significantly reduces viral infection (Han et al., 2006; Hofmann et al., 2006; Li et al., 2005c). In this study, since residue Y217 is unlikely to make direct contact with RBD, it must employ a different mechanism for reducing viral entry. In this case, the loss of infection is likely due to the loss of rh-ACE2 expression rather a block of viral interaction (Figs. 4A and B). Since the introduction of Y217N also has a profound effect on hu-ACE2 (Figs. 6A and B), the function of the mutation is unlikely to be a species-specific phenomenon. We, therefore, believe that we have identified a natural mutation, which is likely critical for a functional domain in regulating the gene expression of both rh-ACE2 and hu-ACE2. Our results also indicate that natural mutations in rh-ACE2 probably play a role in modulating SARS-CoV infection efficiency. However, how exactly the Y217N mutation leads to the reduced expression of both rh-ACE2 and hu-ACE2 will require further investigation.

Materials and methods

Animals

Eleven Chinese macaques were experimentally infected with a pathogenic strain of SARS-CoV, SARS-CoV$_{PUMC01}$ as we described in our previous studies (Chen et al., 2005; Li et al., 2005a; Qin et al., 2005). Tissue specimens collected on day 7 post infection were used for this study to understand the early lung pathology. Two uninfected monkeys were included as controls. The experiment was conducted in our Bio-safety Level 3 animal facility. Our animal protocols were approved by our institutional ethic committee before conducting the experiments. The background information of these animals have been presented in table one.

Pathological evaluation of rhesus specimens

Specimens collected from all seven lung lobes of each infected animal. The severity of lung damage was determined based on previously described criteria (Li et al., 2005a). Briefly, the + to ++ in the six-grade scoring system refer to mild lung damage including alveolar septa broadening, distorted partially, and mild monocyte infiltration in alveolar septa. The +++ to ++++ refer to severe lung damage including DAD, extensive alveolar septa broadening, restricted fusion of thick septa by pressure, ruptured elastic fiber of septa, variably filled with fibrin, erythrocytes, cellular debris, and enhanced infiltration of inflammatory cells in alveolar cavities. For the detection of SARS-CoV viral antigens, we used an immunohistochemical assay as previously described (Li et al., 2005a; Qin et al., 2005).

Rh-ACE2 sequence analysis

Total RNA was isolated from lung and kidney tissues using Trizol (Invitrogen, Carlsbad, CA). cDNA was generated from 1 μg of total RNA using the Protoscript First Strand cDNA Synthesis Kit (NEB, Ipswich, MA) and subjected to PCR to amplify the full-length rhesus ACE2 (Rh-ACE2) gene by nested PCR with primer pairs: external forward 5′-GAGGA GGTTT TAGTC TAGGG AAAGT-3′; external backward: 5′-GAGAA CCTCA CTAAA ACAAC-3′; internal forward:5′-TCGGG GTACC CAGTG TATGT GATCT TGGCT CA-3′; internal backward: 5′-ACAAA AAAGA GAACC TCACT TTCCC CCTT-3′). High fidelity Taq polymerase (Roche, Indianapolis, IN) was used for the reaction. The amplification cycles include: 30 s at 94 °C for 1 cycle; 30 s at 94 °C, 30 s at 58 °C, 2 min and 30 s at 68 °C for 35 cycles, followed by an extension for 10 min at 72 °C using outer primers; then 30 s at 94 °C for 1 cycle; 30 s at 94 °C, 30 s at 58 °C, 2 min and 30 s at 68 °C for 35 cycles, followed by an extension for 10 min at 72 °C using inner primers. The PCR products were subsequently cloned and sequence analyzed. GenBank accession numbers are FJ170076–FJ170101.

Rh-ACE2 mRNA quantification using real-time PCR

One microgram total RNA extracted from monkey's lung tissue was subjected to reverse transcription to generate cDNA. Two μl cDNA of each sample was used to quantify the Rh-ACE2 mRNA with QuantiTect SYBR Green PCR Master Mix (Qiagen, Valencia, CA) in the Real-time LightCycler PCR system (Roche, Indianapolis, IN). As a control, 2 μl cDNA of each sample was also subjected to real-time PCR using GAPDH-specific oligonucleotides. The following primer pairs were used: (i) Rh-ACE2 forward: 5′-GGACC CAGGA AATGT TCAGA-3′ and backward: 5′-GGCTG CAGAA AGTGA CATGA-3′ (15); (ii) GAPDH gene forward: 5′-ACAAC TTTGG CATTG TGGAA-3′ and backward: 5′-GATGC AGGGA TGATG TTCTG-3′. Differences in ACE2 expression were represented as the fold change in gene expression using the $2^{-}\Delta\Delta^{CT}$

method. The housekeeping gene GAPDH was used as the internal control.

Western blot assay

Forty-eight hours post transfection, HEK293T cells were harvested and lysed in lysis buffer (50 mM Tris–HCl [pH 8.0], 137 mM NaCl, 2 mM EDTA, 0.5% NP-40, 10% glycerol, 1 μg/ml each of pepstatin, leupeptin, and pefabloc). Cell lysates were boiled at 100 °C for 10 min and then subjected to 10% tris–glycine gel (Invitrogen, Carlsbad, CA). Proteins were transferred to a PVDF membrane (Invitrogen, Carlsbad, CA) and incubated with blocking buffer (5% milk and 0.05% BSA) overnight. A rabbit anti-human ACE2 polyclonal antibody (ab15348; Abcam, Cambridge, UK) was used to detect the expression of ACE2 as previously described (Chen et al., 2005). The HRP-labeled anti-rabbit IgG (Amersham-Pharmacia, Piscataway, NJ) was used as the secondary antibody.

Immunofluorescence assay

HEK293T cells transfected with ACE2 expression plasmids were washed with PBS and fixed with 100% cold methanol for 10 min at 48 h post transfection. Fixed cells were washed and then incubated with goat anti-human ACE2 antibody (AF933; R and D systems, Minneapolis, MN). The positive cells were detected, after a FITC-conjugated donkey anti-goat IgG (Invitrogen, Carlsbad, CA) staining step, under a fluorescence microscope.

Pseudovirus entry assay

This assay has been described in our previous publications (Chen et al., 2005; Liu et al., 2007; Yi et al., 2005). Briefly, HEK293T cells (1.5×10^5 cells per well) in 6-well plates were transfected with 1 μg ACE2 plasmid (SuperFect Transfection Reagent). On the following day, the transfected cells were diluted to 1.5×10^5 cells/mL and seeded in 96-well plates in a volume of 100 μl per well at 37 °C overnight. Forty-eight hours post transfection, 5 ng pseudotyped virus (based on p24 concentrations) and 16 ng polybrene (in 100 μl medium) were added to the cells. Seventy-two hours after viral inoculation, cells were tested for virus-encoded luciferase activity using proper reagents (Promega, Madison, WI) and measured in a DYNEX REVELATION 4.06 machine.

Mutagenesis of Rh-ACE2 and Hu-ACE2 genes

QuickChange® Site-Directed Mutagenesis System (Stratagene, La Jolla, CA) with PfuUltra™ High-Fidelity DNA polymerase was used to generate mutations in Rh-ACE2 and Hu-ACE2 genes. The amino acid change the nucleotide mutation were performed as follows: G192R: AGA to GGA; N217Y: TAC to AAC. The following primers were used to generate mutants: (i) 11-7 ACE2 (G192R) Forward: 5′-AAAAA TGAGA TGGCA AGAGC AAATC ATTATA-3′ and Backward: 5′-TATAA TGATT TGCTC TTGCC ATCTC ATTTT T-3′, (ii) 11-7 ACE2 (N217Y) Forward: 5′-GTAGA TGGCT ATGAC TACAA CCGCG ACCAGT-3′ and Backward: 5′-ACTGG TCGCG GTTGT AGTCA TAGCC ATCTA C-3′. The amplification parameters used were as follows: 30 s at 95 °C for 1 cycle; 30 s at 95 °C, 1 min at 55 °C, 6 min at 68 °C for 15 cycles. We followed the manufacturer's instruction for the rest of the experiment.

Acknowledgments

We thank Lian Huang, Zhe Cong, Yali Liu, Wei Tong, Yanfeng Xu, Chunmei Ma, Wei Deng, Xiaowei Dai, Xiuhong Yang, Jiamei Li and Chunshi Jia for technical assistance. We also thank the NIH (1R01 HL080211-01 to Z.C.) and the Development Fund of the University of Hong Kong (UDF) to its AIDS Institute for financial support.

References

Chan, V.S., Chan, K.Y., Chen, Y., Poon, L.L., Cheung, A.N., Zheng, B., Chan, K.H., Mak, W., Ngan, H.Y., Xu, X., Screaton, G., Tam, P.K., Austyn, J.M., Chan, L.C., Yip, S.P., Peiris, M., Khoo, U.S., Lin, C.L., 2006. Homozygous L-SIGN (CLEC4M) plays a protective role in SARS coronavirus infection. Nat. Genet. 38 (1), 38–46.

Chen, Z., Zhou, P., Ho, D.D., Landau, N.R., Marx, P.A., 1997. Genetically divergent strains of simian immunodeficiency virus use CCR5 as a coreceptor for entry. J. Virol. 71 (4), 2705–2714.

Chen, Z., Gettie, A., Ho, D.D., Marx, P.A., 1998a. Primary SIVsm isolates use the CCR5 coreceptor from sooty mangabeys naturally infected in west Africa: a comparison of coreceptor usage of primary SIVsm, HIV-2, and SIVmac. Virology 246 (1), 113–124.

Chen, Z., Kwon, D., Jin, Z., Monard, S., Telfer, P., Jones, M.S., Lu, C.Y., Aguilar, R.F., Ho, D.D., Marx, P.A., 1998b. Natural infection of a homozygous delta24 CCR5 red-capped mangabey with an R2b-tropic simian immunodeficiency virus. J. Exp. Med. 188 (11), 2057–2065.

Chen, Z., Zhang, L., Qin, C., Ba, L., Yi, C.E., Zhang, F., Wei, Q., He, T., Yu, W., Yu, J., Gao, H., Tu, X., Gettie, A., Farzan, M., Yuen, K.Y., Ho, D.D., 2005. Recombinant modified vaccinia virus Ankara expressing the spike glycoprotein of severe acute respiratory syndrome coronavirus induces protective neutralizing antibodies primarily targeting the receptor binding region. J. Virol. 79 (5), 2678–2688.

Chiu, R.W., Tang, N.L., Hui, D.S., Chung, G.T., Chim, S.S., Chan, K.C., Sung, Y.M., Chan, L.Y., Tong, Y.K., Lee, W.S., Chan, P.K., Lo, Y.M., 2004. ACE2 gene polymorphisms do not affect outcome of severe acute respiratory syndrome. Clin. Chem. 50 (9), 1683–1686.

Crackower, M.A., Sarao, R., Oudit, G.Y., Yagil, C., Kozieradzki, I., Scanga, S.E., Oliveira-dos-Santos, A.J., da Costa, J., Zhang, L., Pei, Y., Scholey, J., Ferrario, C.M., Manoukian, A.S., Chappell, M.C., Backx, P.H., Yagil, Y., Penninger, J.M., 2002. Angiotensin-converting enzyme 2 is an essential regulator of heart function. Nature 417 (6891), 822–828.

Ding, Y., He, L., Zhang, Q., Huang, Z., Che, X., Hou, J., Wang, H., Shen, H., Qiu, L., Li, Z., Geng, J., Cai, J., Han, H., Li, X., Kang, W., Weng, D., Liang, P., Jiang, S., 2004. Organ distribution of severe acute respiratory syndrome (SARS) associated coronavirus (SARS-CoV) in SARS patients: implications for pathogenesis and virus transmission pathways. J. Pathol. 203 (2), 622–630.

Donnelly, C.A., Fisher, M.C., Fraser, C., Ghani, A.C., Riley, S., Ferguson, N.M., Anderson, R.M., 2004. Epidemiological and genetic analysis of severe acute respiratory syndrome. Lancet. Infect. Dis. 4 (11), 672–683.

Drosten, C., Gunther, S., Preiser, W., van der Werf, S., Brodt, H.R., Becker, S., Rabenau, H., Panning, M., Kolesnikova, L., Fouchier, R.A., Berger, A., Burguiere, A.M., Cinatl, J., Eickmann, M., Escriou, N., Grywna, K., Kramme, S., Manuguerra, J.C., Muller, S., Rickerts, V., Sturmer, M., Vieth, S., Klenk, H.D., Osterhaus, A.D., Schmitz, H., Doerr, H.W., 2003. Identification of a novel coronavirus in patients with severe acute respiratory syndrome. N. Engl. J. Med. 348 (20), 1967–1976.

Franks, T.J., Chong, P.Y., Chui, P., Galvin, J.R., Lourens, R.M., Reid, A.H., Selbs, E., McEvoy, C.P., Hayden, C.D., Fukuoka, J., Taubenberger, J.K., Travis, W.D., 2003. Lung pathology of severe acute respiratory syndrome (SARS): a study of 8 autopsy cases from Singapore. Hum. Pathol. 34 (8), 743–748.

Hamming, I., Timens, W., Bulthuis, M.L., Lely, A.T., Navis, G.J., van Goor, H., 2004. Tissue distribution of ACE2 protein, the functional receptor for SARS coronavirus. A first step in understanding SARS pathogenesis. J. Pathol. 203 (2), 631–637.

Han, D.P., Penn-Nicholson, A., Cho, M.W., 2006. Identification of critical determinants on ACE2 for SARS-CoV entry and development of a potent entry inhibitor. Virology 350 (1), 15–25.

He, L., Ding, Y., Zhang, Q., Che, X., He, Y., Shen, H., Wang, H., Li, Z., Zhao, L., Geng, J., Deng, Y., Yang, L., Li, J., Cai, J., Qiu, L., Wen, K., Xu, X., Jiang, S., 2006. Expression of elevated levels of pro-inflammatory cytokines in SARS-CoV-infected ACE2+ cells in SARS patients: relation to the acute lung injury and pathogenesis of SARS. J. Pathol. 210 (3), 288–297.

Hofmann, H., Simmons, G., Rennekamp, A.J., Chaipan, C., Gramberg, T., Heck, E., Geier, M., Wegele, A., Marzi, A., Bates, P., Pohlmann, S., 2006. Highly conserved regions within the spike proteins of human coronaviruses 229E and NL63 determine recognition of their respective cellular receptors. J. Virol. 80 (17), 8639–8652.

Huang, I.C., Bosch, B.J., Li, F., Li, W., Lee, K.H., Ghiran, S., Vasilieva, N., Dermody, T.S., Harrison, S.C., Dormitzer, P.R., Farzan, M., Rottier, P.J., Choe, H., 2006. SARS coronavirus, but not human coronavirus NL63, utilizes cathepsin L to infect ACE2-expressing cells. J. Biol. Chem. 281 (6), 3198–3203.

Imai, Y., Kuba, K., Rao, S., Huan, Y., Guo, F., Guan, B., Yang, P., Sarao, R., Wada, T., Leong-Poi, H., Crackower, M.A., Fukamizu, A., Hui, C.C., Hein, L., Uhlig, S., Slutsky, A.S., Jiang, C., Penninger, J.M., 2005. Angiotensin-converting enzyme 2 protects from severe acute lung failure. Nature 436 (7047), 112–116.

Itoyama, S., Keicho, N., Hijikata, M., Quy, T., Phi, N.C., Long, H.T., Ha le, D., Ban, V.V., Matsushita, I., Yanai, H., Kirikae, F., Kirikae, T., Kuratsuji, T., Sasazuki, T., 2005. Identification of an alternative 5'-untranslated exon and new polymorphisms of angiotensin-converting enzyme 2 gene: lack of association with SARS in the Vietnamese population. Am. J. Med. Genet. A. 136 (1), 52–57.

Kuba, K., Imai, Y., Rao, S., Gao, H., Guo, F., Guan, B., Huan, Y., Yang, P., Zhang, Y., Deng, W., Bao, L., Zhang, B., Liu, G., Wang, Z., Chappell, M., Liu, Y., Zheng, D., Leibbrandt, A., Wada, T., Slutsky, A.S., Liu, D., Qin, C., Jiang, C., Penninger, J.M., 2005. A crucial role of angiotensin converting enzyme 2 (ACE2) in SARS coronavirus-induced lung injury. Nat. Med. 11 (8), 875–879.

Kuiken, T., Fouchier, R.A., Schutten, M., Rimmelzwaan, G.F., van Amerongen, G., van Riel, D., Laman, J.D., de Jong, T., van Doornum, G., Lim, W., Ling, A.E., Chan, P.K., Tam, J.S., Zambon, M.C., Gopal, R., Drosten, C., van der Werf, S., Escriou, N., Manuguerra, J.C., Stohr, K., Peiris, J.S., Osterhaus, A.D., 2003. Newly discovered coronavirus as the primary cause of severe acute respiratory syndrome. Lancet 362 (9380), 263–270.

Law, H.K., Cheung, C.Y., Ng, H.Y., Sia, S.F., Chan, Y.O., Luk, W., Nicholls, J.M., Peiris, J.S., Lau, Y.L., 2005. Chemokine up-regulation in SARS-coronavirus-infected, monocyte-derived human dendritic cells. Blood 106 (7), 2366–2374.

Li, W., Moore, M.J., Vasilieva, N., Sui, J., Wong, S.K., Berne, M.A., Somasundaran, M., Sullivan, J.L., Luzuriaga, K., Greenough, T.C., Choe, H., Farzan, M., 2003. Angiotensin-converting enzyme 2 is a functional receptor for the SARS coronavirus. Nature 426 (6965), 450–454.

Li, B.J., Tang, Q., Cheng, D., Qin, C., Xie, F.Y., Wei, Q., Xu, J., Liu, Y., Zheng, B.J., Woodle, M.C., Zhong, N., Lu, P.Y., 2005a. Using siRNA in prophylactic and therapeutic regimens against SARS coronavirus in Rhesus macaque. Nat. Med. 11 (9), 944–951.

Li, F., Li, W., Farzan, M., Harrison, S.C., 2005b. Structure of SARS coronavirus spike receptor-binding domain complexed with receptor. Science 309 (5742), 1864–1868.

Li, W., Zhang, C., Sui, J., Kuhn, J.H., Moore, M.J., Luo, S., Wong, S.K., Huang, I.C., Xu, K., Vasilieva, N., Murakami, A., He, Y., Marasco, W.A., Guan, Y., Choe, H., Farzan, M., 2005c. Receptor and viral determinants of SARS-coronavirus adaptation to human ACE2. EMBO. J. 24 (8), 1634–1643.

Li, F., Berardi, M., Li, W., Farzan, M., Dormitzer, P.R., Harrison, S.C., 2006. Conformational states of the severe acute respiratory syndrome coronavirus spike protein ectodomain. J. Virol. 80 (14), 6794–6800.

Liu, L., Fang, Q., Deng, F., Wang, H., Yi, C.E., Ba, L., Yu, W., Lin, R.D., Li, T., Hu, Z., Ho, D.D., Zhang, L., Chen, Z., 2007. Natural mutations in the receptor binding domain of spike glycoprotein determine the reactivity of cross-neutralization between palm civet coronavirus and severe acute respiratory syndrome coronavirus. J. Virol. 81 (9), 4694–4700.

Mossel, E.C., Huang, C., Narayanan, K., Makino, S., Tesh, R.B., Peters, C.J., 2005. Exogenous ACE2 expression allows refractory cell lines to support severe acute respiratory syndrome coronavirus replication. J. Virol. 79 (6), 3846–3850.

Nicholls, J.M., Poon, L.L., Lee, K.C., Ng, W.F., Lai, S.T., Leung, C.Y., Chu, C.M., Hui, P.K., Mak, K.L., Lim, W., Yan, K.W., Chan, K.H., Tsang, N.C., Guan, Y., Yuen, K.Y., Peiris, J.S., 2003. Lung pathology of fatal severe acute respiratory syndrome. Lancet 361 (9371), 1773–1778.

Osterhaus, A.D., Fouchier, R.A., Kuiken, T., 2004. The aetiology of SARS: Koch's postulates fulfilled. Philos. Trans. R. Soc. Lond. B. Biol. Sci. 359 (1447), 1081–1082.

Peiris, J.S., Chu, C.M., Cheng, V.C., Chan, K.S., Hung, I.F., Poon, L.L., Law, K.I., Tang, B.S., Hon, T.Y., Chan, C.S., Chan, K.H., Ng, J.S., Zheng, B.J., Ng, W.L., Lai, R.W., Guan, Y., Yuen, K.Y., 2003a. Clinical progression and viral load in a community outbreak of coronavirus-associated SARS pneumonia: a prospective study. Lancet 361 (9371), 1767–1772.

Peiris, J.S., Yuen, K.Y., Osterhaus, A.D., Stohr, K., 2003b. The severe acute respiratory syndrome. N. Engl. J. Med. 349 (25), 2431–2441.

Peiris, J.S., Guan, Y., Yuen, K.Y., 2004. Severe acute respiratory syndrome. Nat. Med. 10 (12 Suppl), S88–97.

Qin, C., Wang, J., Wei, Q., She, M., Marasco, W.A., Jiang, H., Tu, X., Zhu, H., Ren, L., Gao, H., Guo, L., Huang, L., Yang, R., Cong, Z., Wang, Y., Liu, Y., Sun, Y., Duan, S., Qu, J., Chen, L., Tong, W., Ruan, L., Liu, P., Zhang, H., Zhang, J., Liu, D., Liu, Q., Hong, T., He, W., 2005. An animal model of SARS produced by infection of Macaca mulatta with SARS coronavirus. J. Pathol. 206 (3), 251–259.

Riley, S., Fraser, C., Donnelly, C.A., Ghani, A.C., Abu-Raddad, L.J., Hedley, A.J., Leung, G.M., Ho, L.M., Lam, T.H., Thach, T.Q., Chau, P., Chan, K.P., Lo, S.V., Leung, P.Y., Tsang, T., Ho, W., Lee, K.H., Lau, E.M., Ferguson, N.M., Anderson, R.M., 2003. Transmission dynamics of the etiological agent of SARS in Hong Kong: impact of public health interventions. Science 300 (5627), 1961–1966.

Rowe, T., Gao, G., Hogan, R.J., Crystal, R.G., Voss, T.G., Grant, R.L., Bell, P., Kobinger, G.P., Wivel, N.A., Wilson, J.M., 2004. Macaque model for severe acute respiratory syndrome. J. Virol. 78 (20), 11401–11404.

Shieh, W.J., Hsiao, C.H., Paddock, C.D., Guarner, J., Goldsmith, C.S., Tatti, K., Packard, M., Mueller, L., Wu, M.Z., Rollin, P., Su, I.J., Zaki, S.R., 2005. Immunohistochemical, in situ hybridization, and ultrastructural localization of SARS-associated coronavirus in lung of a fatal case of severe acute respiratory syndrome in Taiwan. Hum. Pathol. 36 (3), 303–309.

Sims, A.C., Baric, R.S., Yount, B., Burkett, S.E., Collins, P.L., Pickles, R.J., 2005. Severe acute respiratory syndrome coronavirus infection of human ciliated airway epithelia: role of ciliated cells in viral spread in the conducting airways of the lungs. J. Virol. 79 (24), 15511–15524.

To, K.F., Tong, J.H., Chan, P.K., Au, F.W., Chim, S.S., Chan, K.C., Cheung, J.L., Liu, E.Y., Tse, G.M., Lo, A.W., Lo, Y.M., Ng, H.K., 2004. Tissue and cellular tropism of the coronavirus associated with severe acute respiratory syndrome: an in-situ hybridization study of fatal cases. J. Pathol. 202 (2), 157–163.

Tse, G.M., To, K.F., Chan, P.K., Lo, A.W., Ng, K.C., Wu, A., Lee, N., Wong, H.C., Mak, S.M., Chan, K.F., Hui, D.S., Sung, J.J., Ng, H.K., 2004. Pulmonary pathological features in coronavirus associated severe acute respiratory syndrome (SARS). J. Clin. Pathol. 57 (3), 260–265.

Yi, C.E., Ba, L., Zhang, L., Ho, D.D., Chen, Z., 2005. Single amino acid substitutions in the severe acute respiratory syndrome coronavirus spike glycoprotein determine viral entry and immunogenicity of a major neutralizing domain. J. Virol. 79 (18), 11638–11646.